Automated RSO Stability Analysis

Thomas M. Johnson
Analytical Graphics, Inc., 220 Valley Creek Blvd, Exton, PA 19468, USA

ABSTRACT

A methodology for assessing the attitude stability of a Resident Space Object (RSO) using visual magnitude data is presented and then scaled to run in an automated fashion across the entire satellite catalog. Results obtained by applying the methodology to the Commercial Space Operations Center (COMSpOC) catalog are presented and summarized, identifying objects that have changed stability. We also examine the timeline for detecting the transition from stable to unstable attitude

1. INTRODUCTION

Resident Space Object (RSO) visual magnitude data has been historically difficult to obtain, limited to those participating in dedicated observation campaigns organized by academia, civil space agencies (NASA, ESA, JAXA, etc.), or elements of the US government (AFRL, AFSPC, etc.). This issue is quickly going away in recent years with the significant growth of small telescopes deployed by commercial companies such as Exo Analytics, Inc. and Las Cumbres Observatory Global Telescope network. The partnership between these companies and AGI's Commercial Space Operations Center (ComSpOC) inspired us to examine ways to combine their use astrometric and magnitude data to do large scale analysis across all objects in a catalog.

RSO stability analysis is ideally performed by collecting long duration tracks over several hours a night with each track consisting of a measurement every 2-60 seconds. One model for RSO visual magnitude is shown below [1]

$$\begin{aligned} \mathrm{m_v} &= -26.7 - 2.5\log\big(\mathrm{A\rho F(\phi)}\big) + 5\log(\mathrm{r}) \\ A &= \text{cross-sectional area} \\ \rho &= \text{albedo} \\ r &= \text{range to the object} \\ F &= \frac{1}{4\pi}\,(\text{specular sphere}) \text{ or} \\ &= \frac{2}{3\pi^2}\left[(\pi-\phi)cos\phi + sin\phi\right] \text{ (lambertian sphere)} \end{aligned} \tag{1}$$

The magnitude depends on the observed area, the material properties, and range to the RSO. The RSO shape, material properties, and attitude stability can then be assessed as the analyst looks for higher frequency content in the magnitude data to indicate tumbling and a rotation speed. This level of analysis requires long periods of observation time dedicated to each RSO, often across multiple nights [2, 3, 4, 6]. Collecting magnitude data over a year or longer supports analysis of the RSO under different sensor and lighting geometries to build fingerprints of objects of interest [5]. However there's a tradeoff between dwell time on a given RSO and collecting against multiple RSOs. We are trying to mitigate that trade off by introducing an analytical method that can work with multiple short collects.

The ComSpOC and its sensor partners routinely collect optical tracking data on many RSOs, but other than selected high interest RSOs these collections are short duration tracks lasting just a few minutes. The primary goal is to obtain astrometric data to support catalog maintenance and space situational awareness of the RSO's orbit and maneuver behavior. The track collection frequency varies from 1-2 tracks a night to as often as 10-15 depending on the nature and history of the RSO. At first glance this collection frequency does not appear to be well suited for stability analysis, but our experiments have shown that is possible, albeit with some limitations.

This paper introduces a methodology for exploiting short duration track magnitude information to perform stability analysis and identify RSOs worthy of a more detailed assessment using longer duration tracks. RSO's that transition

from stable to unstable (or vice versa) are of particular interest as this may suggest an on-orbit failure or other change in operational behavior.

2. HYPOTHESIS

A three-axis stabilized RSO in geosynchronous orbit has a relative body orientation to the sensor that changes very little over the course of night as the body is typically nadir pointing by design. The magnitude variation is driven by the changing orientation of the solar panels (sun tracking) or other deployed elements (steerable antennas, etc.) and the differences in material properties as the RSO is lit from different sides. As a result the magnitude data varies slowly throughout the night. The signature is generally repeatable from night to night and from season to season over a year. Spin stabilized RSOs exhibit a similar signature since they are stable in 2 axes and the spin axes is relatively perpendicular to the observer (ignoring the seasonal Sun declination angle variation).

We can therefore assess the RSO's attitude stability by looking at the frequency content of the magnitude data. If the object is three-axis stabilized we expect to see a strong low frequency signature. An unstable object will not have this signature, but may instead show high frequency content. Low and high frequency are relative to the expected variation of the course of one night. We can then repeatedly evaluate the frequency content over a long period of time to produce a classic waterfall plot and use this to assess whether the object's stability is changing.

2.1 Challenges

Frequency analysis is classically performed using standard signal processing methods such as Discrete Fourier Transform (DFT) to produce a periodogram or power spectrum plot. Unfortunately visual magnitude data has some unique characteristics that are not present in a standard signal processing problems:

- Data is not evenly spaced – this is typically driven by the sensor integration time. Typically the sensor integration time is constant during a track but not all frames may be usable, leading to irregularly spaced points.

- Multiple sensors may be observing at the same time but are not typically synchronized. This introduces overlapping measurement time grids sets. Each sensor also has its own integration time.

- The sensors can only operate under the proper lighting conditions (e.g. the RSO is "lit" and the sensor is "in darkness") and when the RSO is in view of the sensor geometrically (e.g. above the horizon).

- The sensor may be unable to observe due to weather or sensor maintenance issues.

It's tempting to try to avoid these problems by resampling (interpolation) or extrapolating the observed data to obtain a nice regularly spaced measurement grid. But you should be very cautious in your treatment of "missing" data between tracks or between nights. The absence of data is not the same as saying that the data points are zero (or other assumed value). .

2.2 Lomb-Scargle Periodogram

The traditional astronomy community has been dealing with these same issues for many years and has developed approaches for dealing with them. One of the primary analysis tools employed is known as the Lomb-Scargle Periodogram [7, 8]. Our analysis is based on this technique. Others [4] have also examined the use of the Lomb-Scargle technique and found it suitable in many cases.

The classic DFT approach calculates the cosine and sine amplitude coefficients on a regularly spaced frequency grid (determined by the sampling frequency and number of sample points). A DFT based periodogram illustrates the relative power level at each of the sample frequencies. The Lomb-Scargle algorithm allows the analyst to pick a set of frequencies of interest and performs a least squares fit at each frequency to determine the cosine and sine amplitude coefficients. Since it's simply choosing a frequency and solving for the coefficients that best fit the observed data points it eliminates the need for the measurements to be regular spaced in time and allows for large gaps in the data set.

We can calculate the Lomb-Scargle periodogram over a span of magnitude data and use the observed frequency content to assess the satellite stability. Before processing the data we remove any constant bias so that the strong frequency component at zero frequency doesn't bleed into our frequencies of interest. Stable RSO attitude orientation and visual magnitude varies on the same order as one orbit period which suggests the frequencies of interest. We calculate the RSO's orbit period T using a recent state vector and generate a set of evenly spaced periods of interest T_i from 0 to 1.5T. The period samples are transformed into the frequency domain to define our sample frequencies.

Note that the sample frequencies are not evenly spaced, nor is there a constraint on the number of frequencies that can be analyzed. But, like a traditional DFT based approach you can't extract more frequency content than the underlying measurement spacing supports. The DFT is limited by the measurement sampling and Nyquist's theorem. A Lomb-Scargle analysis has an absolute frequency limit governed by the minimum spacing between any two points. This topic is addressed in more detail in [9].

2.3 Error Sources

There are a number of potential errors sources that we considered in our analysis:

- Obs association
- Measurement white noise
- Range correction

The first one is the most concerning – from track to track and night to night are we sure that we actually observed the same object? We mitigate this by leveraging the high accuracy orbit solutions and observation association algorithms within AGI's SSA Software Suite as used within the ComSpOC. The magnitude measurement white noise errors are typically around 0.05 (1σ). This is sensor dependent but is a reasonable baseline value.

The magnitude varies with the range from the sensor to the RSO. From equation 1 we can solve for the magnitude difference introduced by a range variation

$$\Delta m_{range} = 5 \log\left(\frac{r_1}{r_2}\right) \tag{2}$$

where r_1 and r_2 are the two different ranges. A sensor observing a typical GEO RSO directly overhead (zenith) versus one on the horizon has

$$\begin{aligned} \mathrm{r}_{zenith} &= 35786 \text{ km} \\ r_{horizon} &= 41679 \text{ km} \\ \Delta \mathrm{m}_{range} &= 5 \log\left(\frac{\mathrm{r}_{zenith}}{\mathrm{r}_{horizon}}\right) = -0.33 \end{aligned} \tag{3}$$

Practically speaking an optical telescope rarely observes all the way down to the horizon. A typical operating limit is a ground elevation angle of 20 degrees yielding

$$\Delta \mathrm{m}_{range} = 5 \log\left(\frac{\mathrm{r}_{zenith}}{\mathrm{r}_{slant}}\right) = -0.22 \tag{4}$$

The range variation isn't significant relative to the attitude variation so we chose to ignore it and treat it as "noise." The error is clearly correlated though and not a true Gaussian error source. But it's convenient to treat it as such with

$$\sigma_{range} = \frac{|-0.22|}{6} = 0.037 \tag{5}$$

It's worth noting the range sigma is of the same order of magnitude as the sensor white noise. If the range varied more significantly such as when tracking an RSO in a highly elliptical orbit then the proper range corrections should be applied to normalize the magnitude data before further processing. For high altitude circular orbits the magnitude

variation due to range from sensor to sensor is minimal. Treating the range and measurement errors as independent Gaussian sources gives us an expected error statistics of

$$\sigma = \sqrt{\sigma_{range}^2 + \sigma_{WN}^2} = 0.062 \tag{6}$$

3. SIMULATED RESULTS

We simulated several situations to test the hypothesis and implementation. Figures 1a and 1b illustrate the behavior of a sinusoid (as seen in the equation below) with a period of 1 day and the same signal with half the data available during the "night." Sample measurements were generated every 5 minutes. This simple model produces a periodic visual magnitude signature similar to observed on-orbit patterns on known stable objects.

$$y(t) = 14 - 2\sin\left(2\pi\frac{t}{T}\right) \tag{7}$$

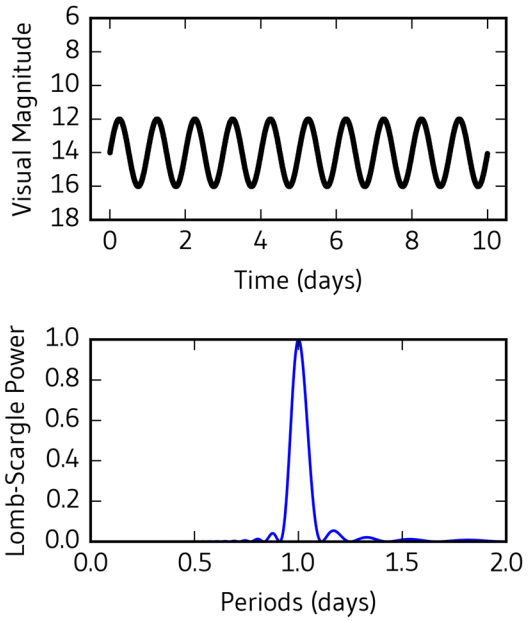

Fig. 1a. Sine Signal

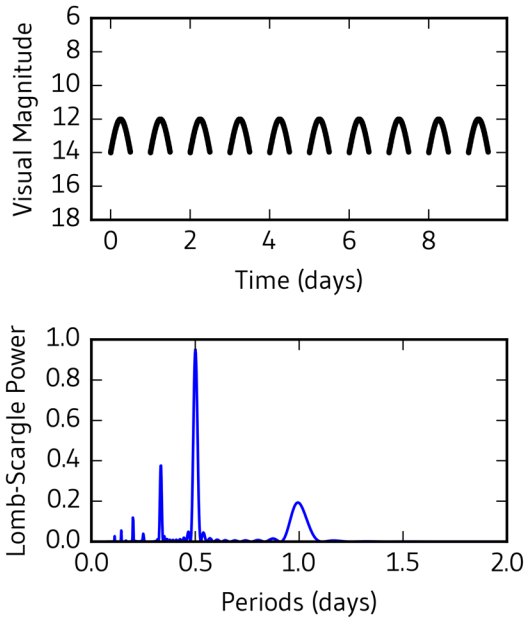

Fig. 1b. "Nightly" Sine Signal

The strong peak at a period of 1 day in Fig 1a is expected. The Fig. 1b results were initially quite surprising – we see a much reduced peak at 1 day and additional peaks at 0.5 and 0.33 days. After further review we realized that when the signal is detrended to remove the mean value the new analysis signal is not a sine wave and the existence of additional peaks should be expected. The addition of white noise ($\sigma_{WN} = 0.1$) to the nightly sine signal has little impact on the frequency signature (Fig. 2a) and a nightly constant value signal with white noise shows no frequency content (Fig 2b), as expected. The signature peaks at 0.5 and 0.33 days remain visible even when $\sigma_{WN} = 1$ (although the peak amplitude are smaller).

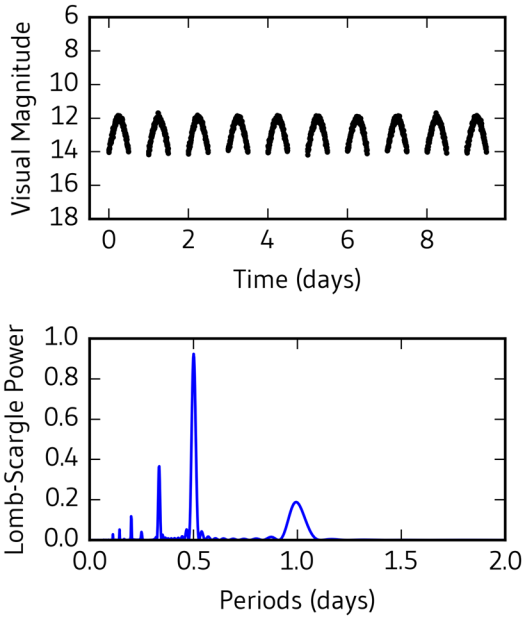

Fig. 2a. "Nightly Sine + Noise Signal

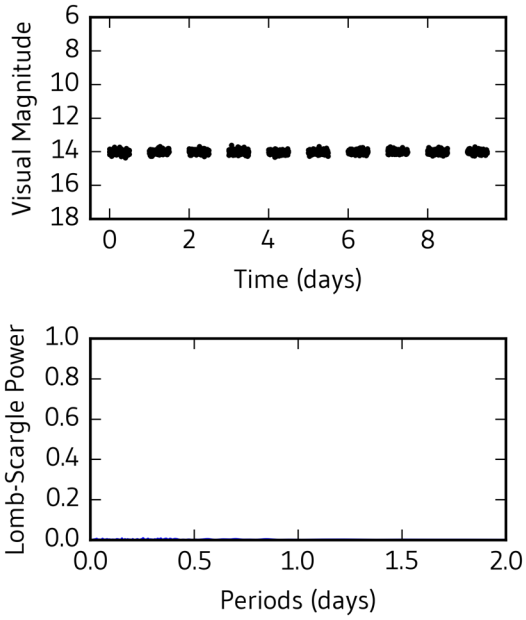

Fig. 2b. Constant + Noise Signal

The test signals examined so far have had data available all night long – in practice this is never the case. We can simulate a more realistic schedule using the following algorithm.

- A track has measurements every 30 seconds.
- The track duration varies uniformly between 1 and 5 minutes (modeled as a discrete uniform random draw between 1 and 6).
- The number of tracks a night varies uniformly between 0 and 4 (modeled as a discrete uniform random draw between 0 and 4).
- Track spacing within a night is random.

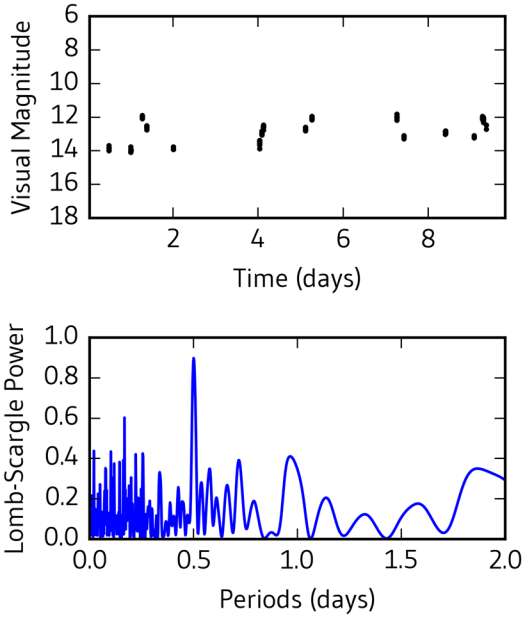

Fig. 3a. Tracks per Night in U[0.4]

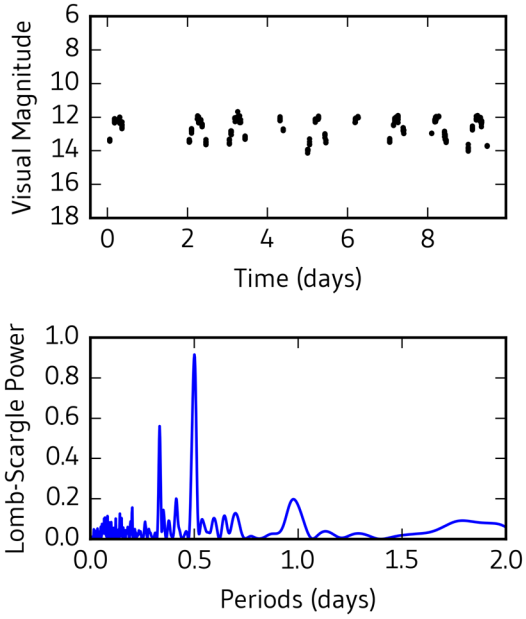

Fig. 3b. "Tracks per Night in U[0, 9]

The peak in Fig. 3a at 0.5 days is still clearly visible. Fig 3b illustrates another run where the number of tracks a night is varied from 0 to 9 - the desired signature is very visible. We perturbed the parameters to determine which were most significant for obtaining a clean frequency signature. Unsurprisingly it's the number of tracks per night and not the measurement density or track duration (all other things being equal). Care should be taken to collect tracks throughout an orbit in order to get a proper sampling of the overall magnitude signature. Overall, the longer the analysis time span the more tracks and points we'll get and the better the frequency resolution will be (narrower peaks). The underlying assumption though is that the object's stability (good or bad) hasn't changed during the analysis span. We'll see examples later on where this is not the case.

The test runs using a well behaved representative signal gives us confidence that the signature can be observable using real world tracks, even under relatively sparse conditions.

4. OBSERVED RESULTS

Analyses were performed using measurements on several RSOs whose stability is known a-priori (or hypothesized):

- Fig. 4 shows GALAXY-15 (SSN ID 28884), an active three-axis stabilized communications RSO in geostationary orbit. It's well tracked because it also serves as a sensor calibration satellite since it hosts a Wide Area Augmentation System (WAAS) payload [CITE TJ CAL PAPER]. The analysis period was 30 days in the Spring of 2016. The first subplot is a graph of all the magnitude data. The second subplot is the same, but with the time axis folded over a duration of one orbit period. The daily periodic signature is evident in this plot and the overall shape supports the use of our original test signal. The last two subplots show the frequency content. The signature peaks are evident in the long-term periodogram, indicating the object is stable. Note how narrow the peaks are since we have a large number of data points to work with. The short-term periodogram shows no significant high frequency content.

- Fig. 5 shows a similar plot for TDRS 3. It's in an inclined GEO orbit but still shows a strong signal of being 3-axis stabilized.

- Fig. 5 shows a similar plot for INMARSAT 3-F4. This data was obtained after it was boosted into a supersync orbit for disposal. It's assumed that after all the on-board systems were turned off that the object began to tumble. The periodogram signatures are quite flat, supporting this hypothesis.

- Fig. 6 shows the results for sparsely tracked GAOFEN-4. This is an imagery satellite in GEO orbit and believed to be 3-axis stabilized. The long-term periodogram signature supports this hypothesis.

- Fig. 7 shows the results for BRASILSAT B1 (SSN 23199), a sparsely tracked, retired communications satellite in supersync orbit. One might expect that this object is tumbling, but the long-term periodogram suggests that it has some stability. This spacecraft was built on a Hughes (now Boeing) HS-376 satellite bus. The HS-376 bus is spin stabilized at 50 RPM in active operations. It's not known whether it kept the spin rate after disposal or was despun as part of the disposal process. No spin rate is observable in the short term periodogram, but this may simply be because it's spinning to fast to be properly sampled with the sensor integration time. Another explanation is that the cylindrical body shape and symmetrical material properties are such that the spin rate does not induce a significant magnitude variation.

- Fig. 8 shows the results for DELTA 4 R/B (SSN 40102). The long term periodogram indicates some stability and the short term periodogram indicates a spin rate of ~ 5 RPM.

- Fig. 9 shows the results for AMOS-5 (SSN 37950), a 3-axis stabilized communication satellite in GEO orbit that failed on November 25, 2015. The results are divided into the pre and post failure sets. The pre-failure data shows its 3 axis stabilized and the post failure data shows it's not.

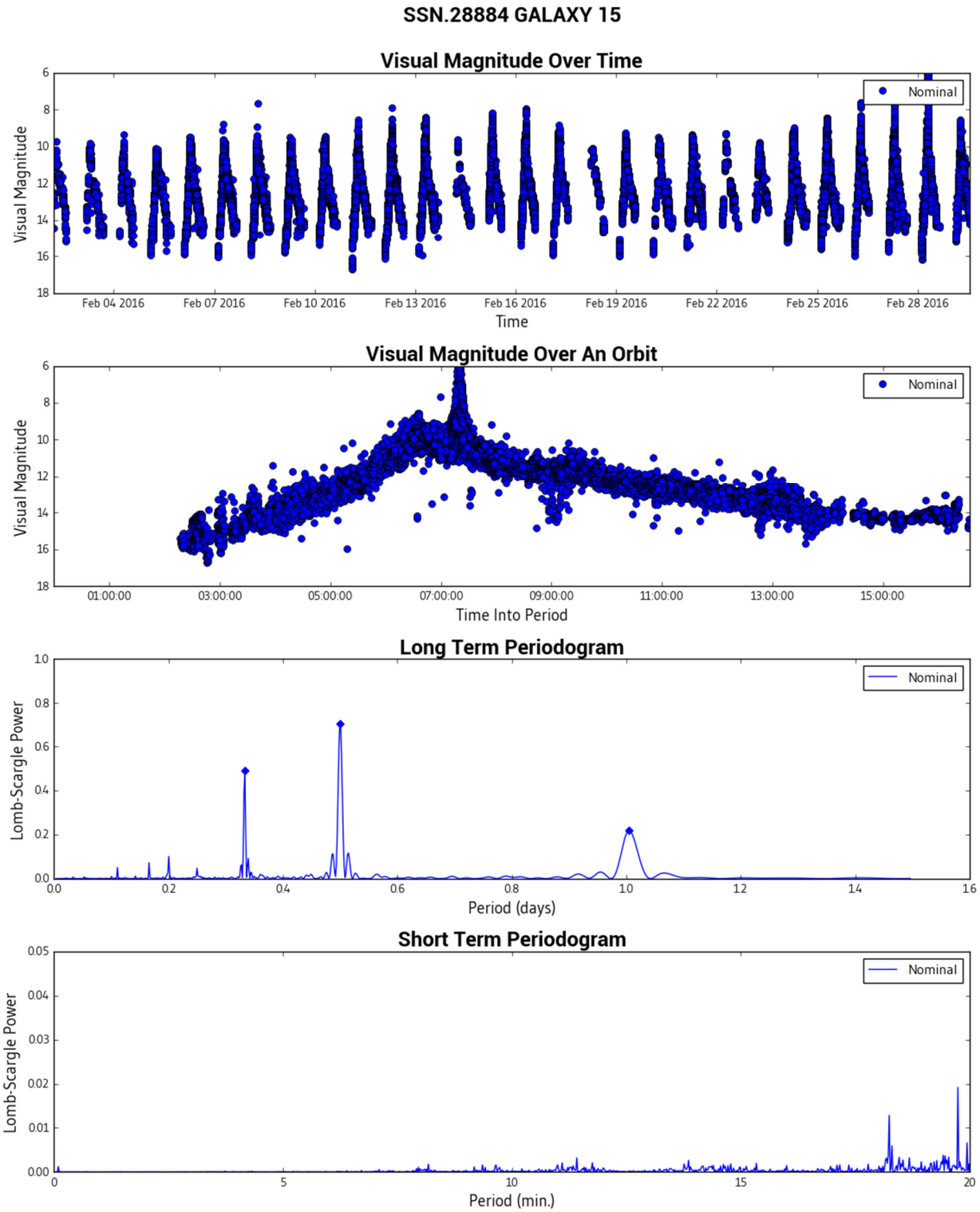

Fig. 4. GALAXY-15. 3-Axis Stabilized in GEO Orbit

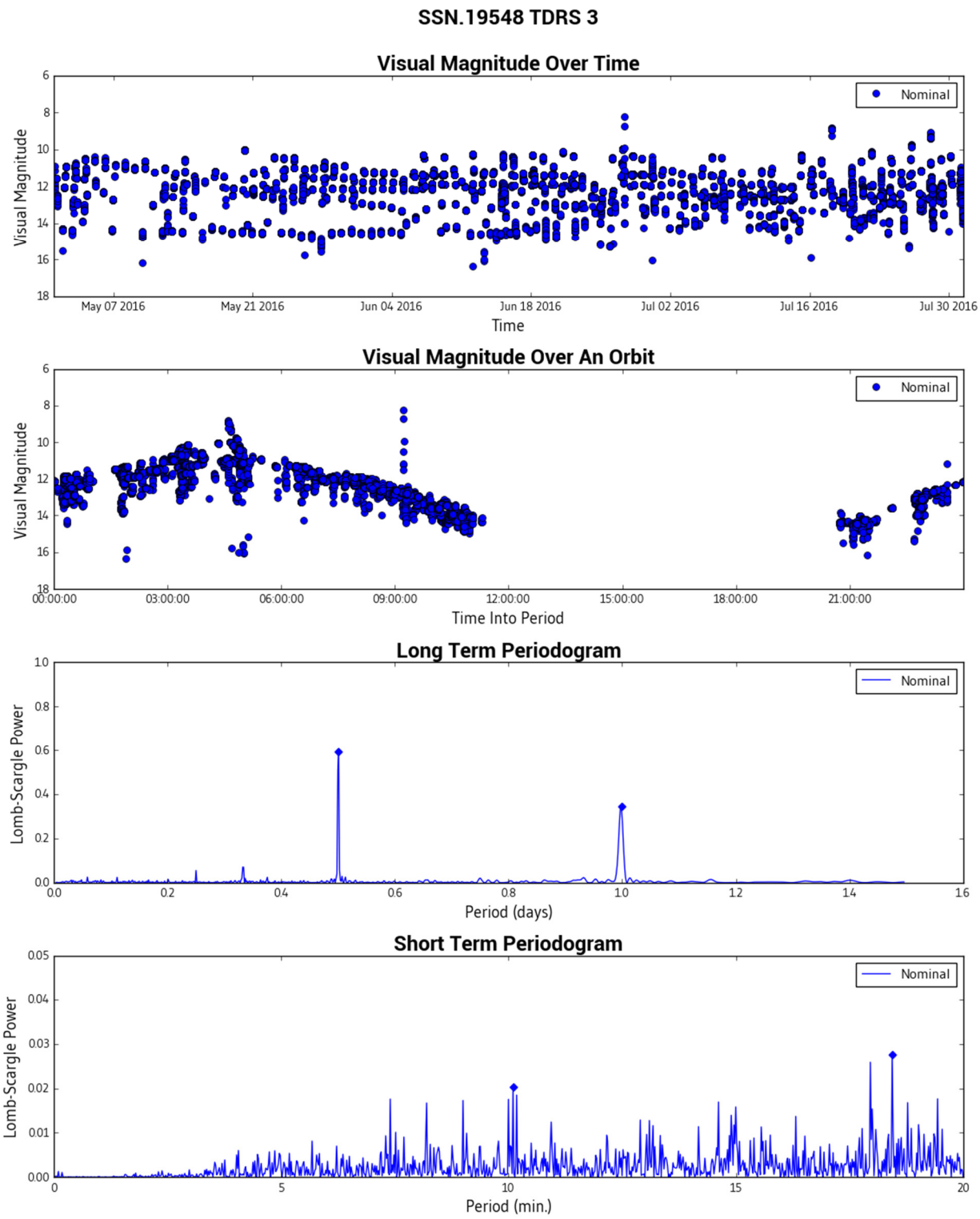

Fig. 4. TDRS 3-Axis Stabilized in Inclined GEO Orbit

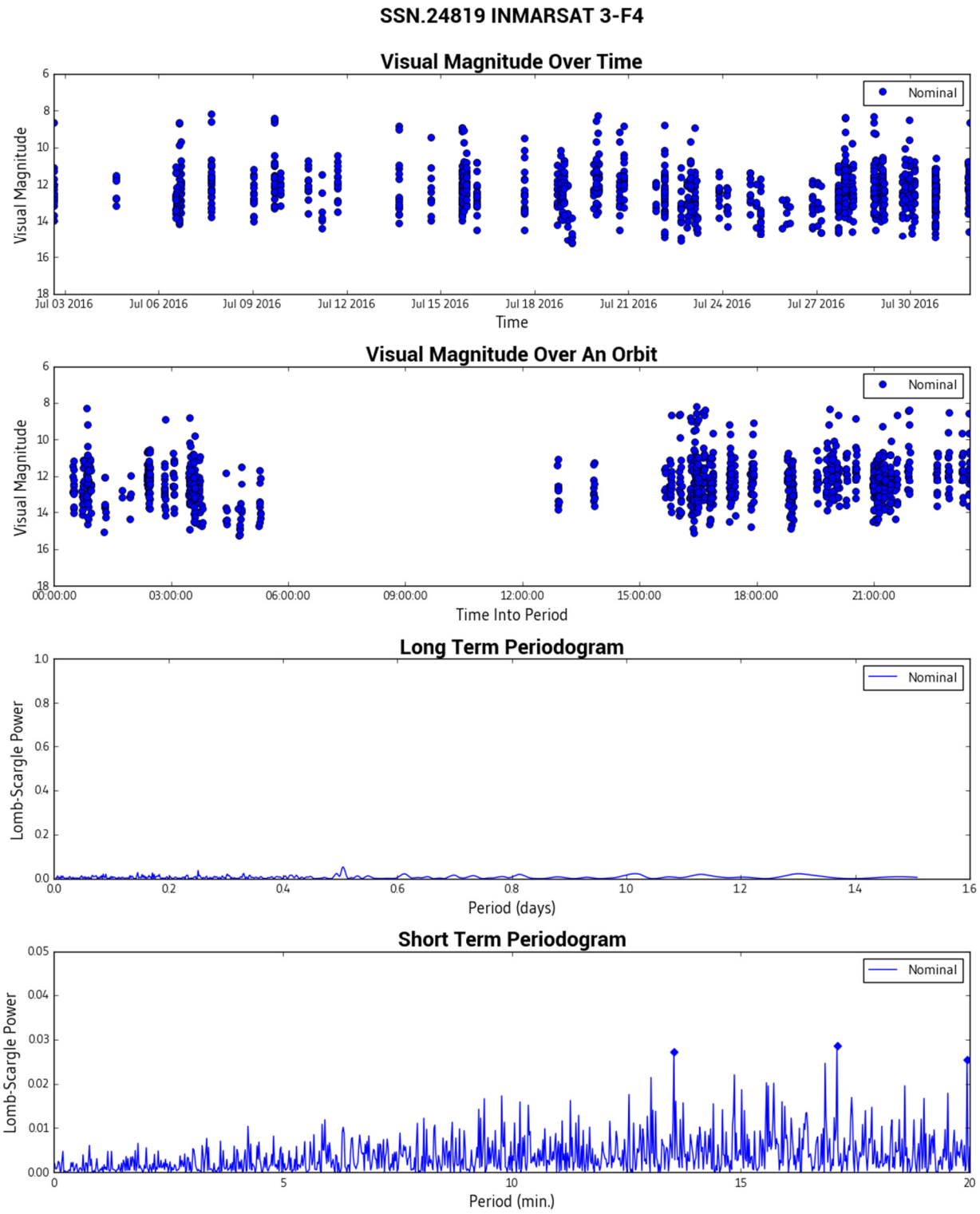

Fig. 5. INMARSAT 3-F4 Tumbling in Supersync Orbit

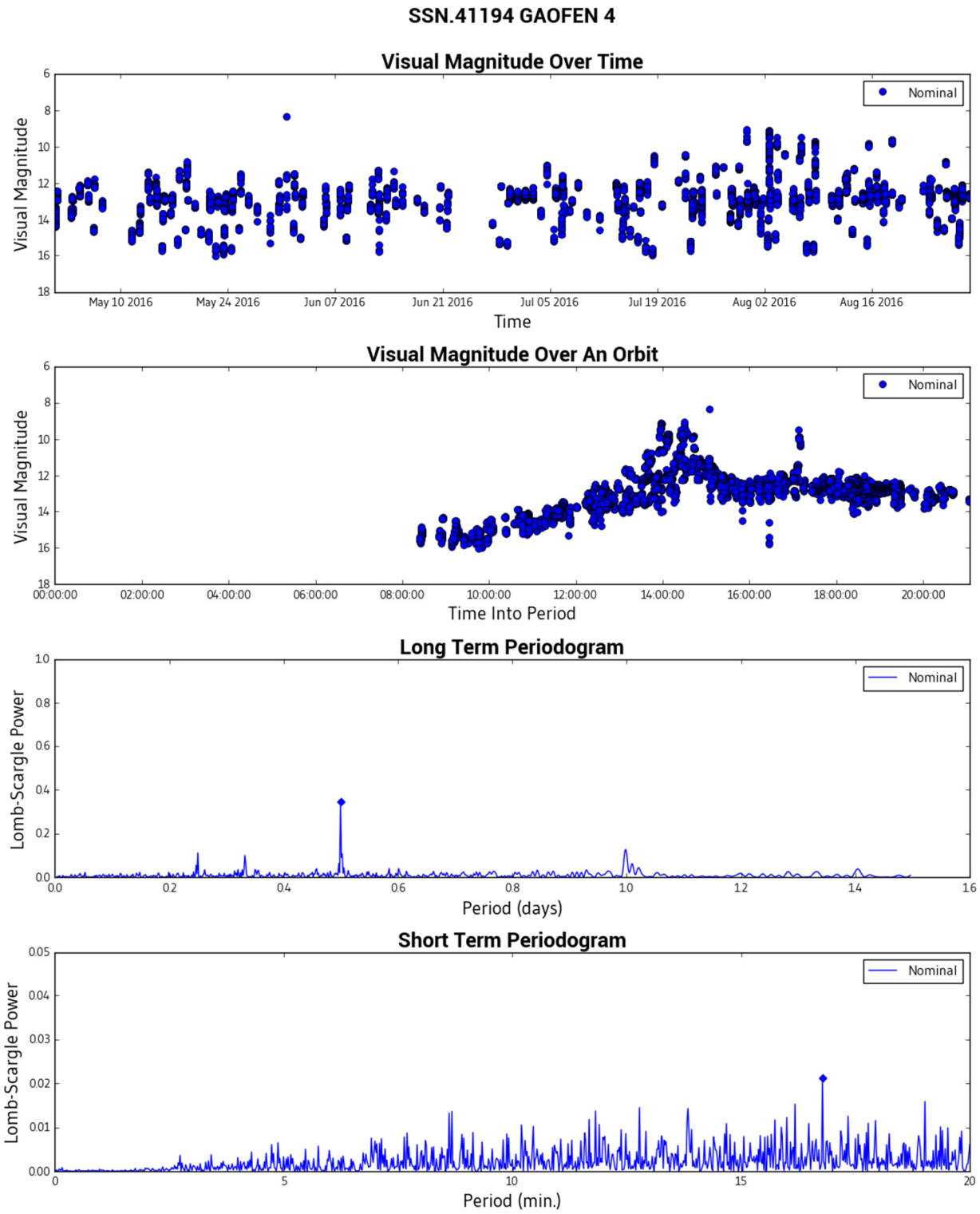

Fig. 6. GAOFEN-4

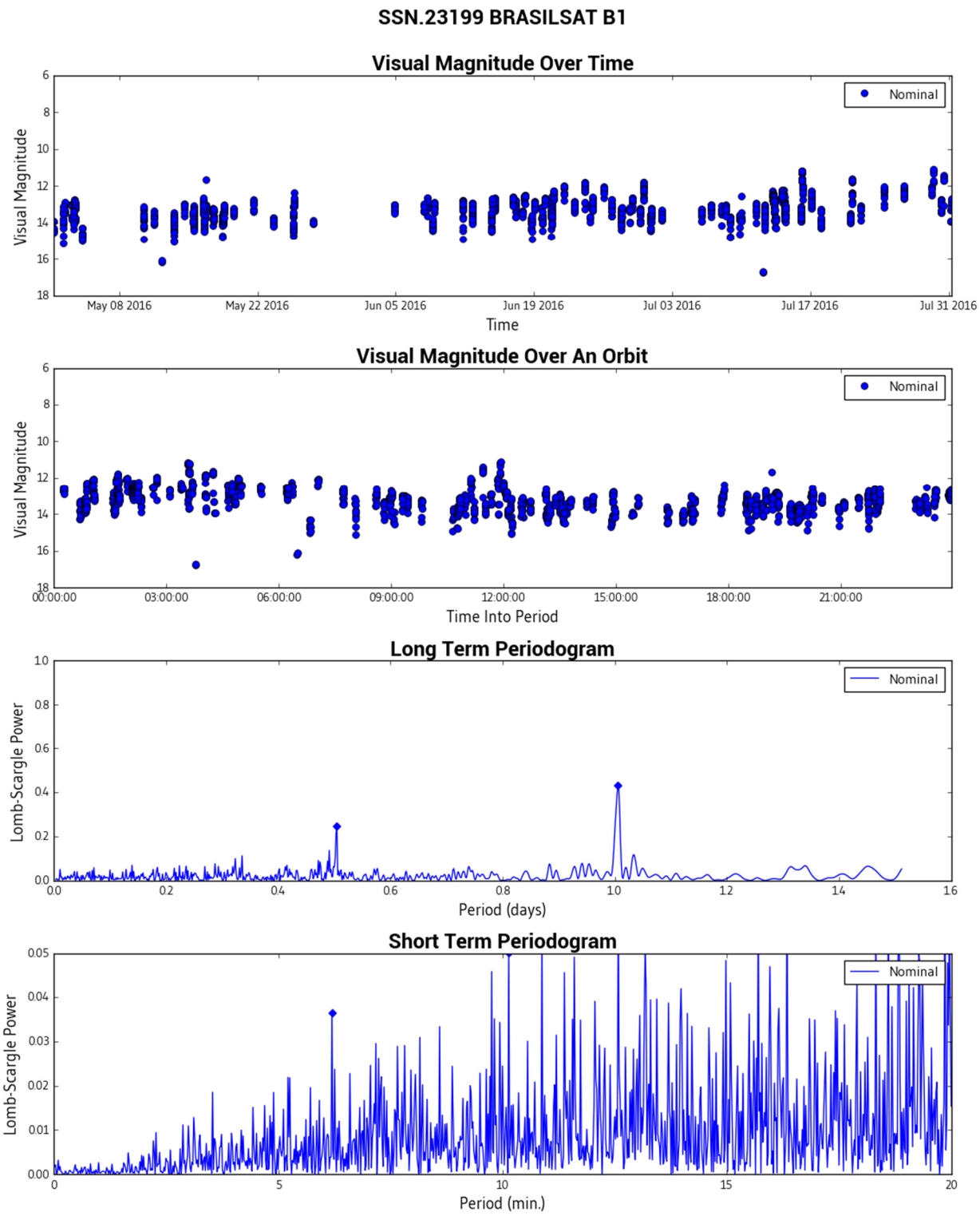

Fig. 7. BRASILSAT B1. Spin Stabilized?, Super Sync GEO.

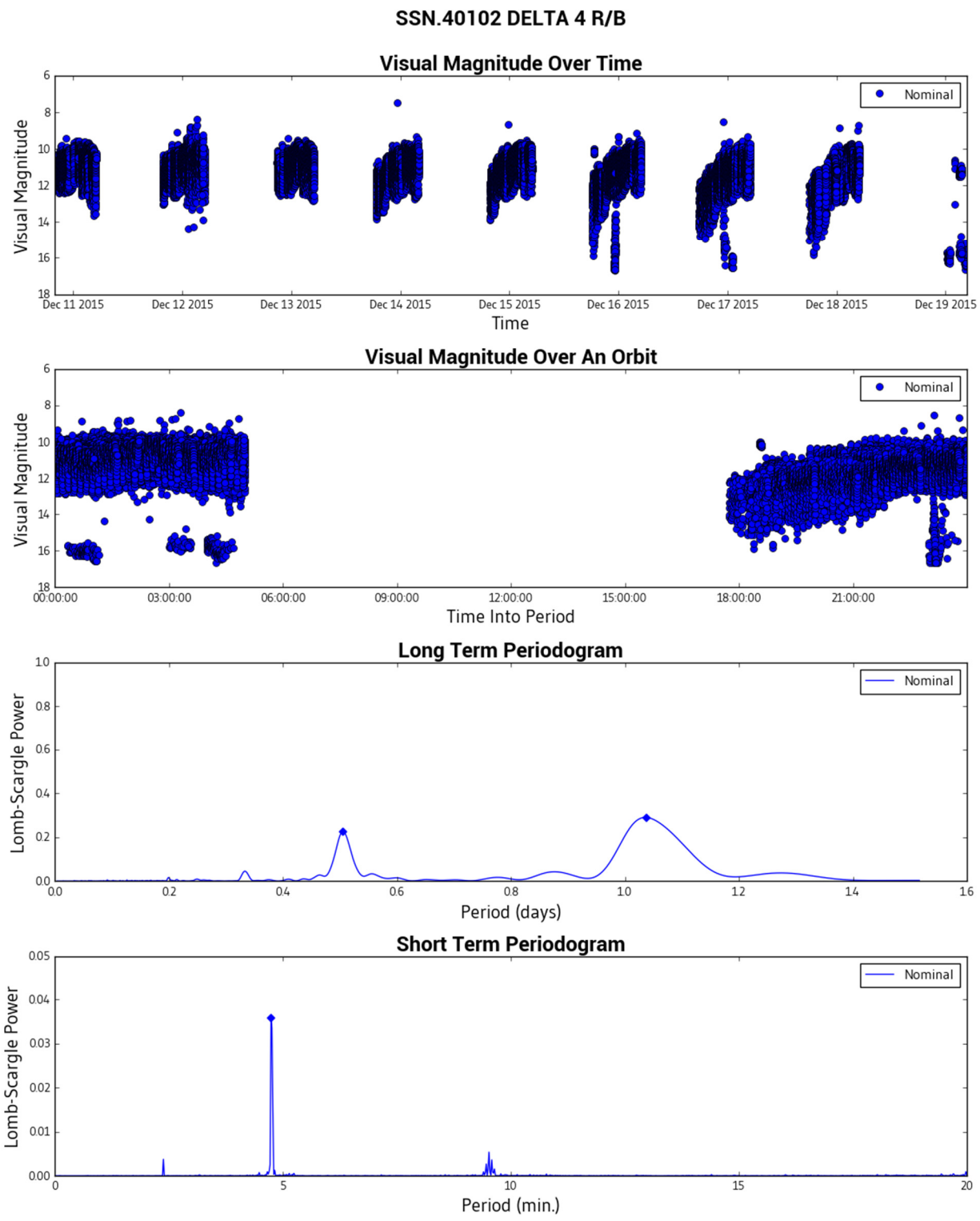

Fig. 8. DELTA-4 R/B. Inertially Stable With a Period of ~5 min.

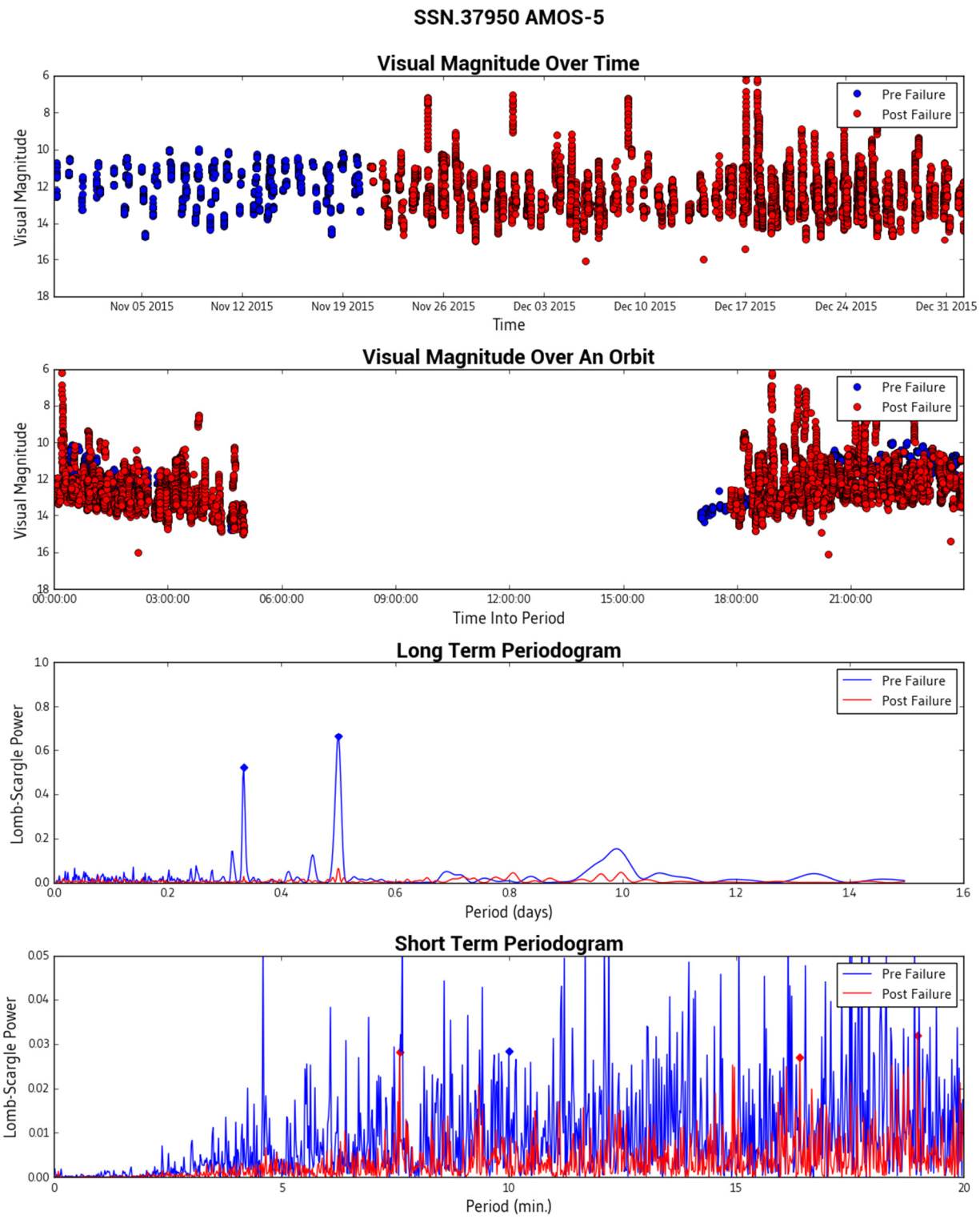

Fig. 9. AMOS-5. Pre and Post Failure Stability

We can expand the analysis method to look at how the RSO's stability evolves over time by building a classic spectrogram or "waterfall" display showing the frequency content as a function of time. This is done by applying the

Lomb-Scargle methodology across sliding time window of data. The time windows overlap each other by an analyst defined percentage. The analyst defines the window length and overlap percentage and has to tradeoff between long windows (to get good frequency resolution) and short windows (to detect changes in frequency content in a rapid fashion). Fig. 10 shows the results for INMARSAT 3-F4 using a sliding window length of 20 days and an overlap of 20%. Notice the typical peaks at 0.5 and 0.33 days. The peaks disappear near the end of April, 2016. This RSO is known to have been supersynced on 1 May 2016 as part of a standard end of life disposal process. The subplot on the right hand side indicates how many measurement samples were used in each window. The results suggest that after completing disposal the RSO is no longer stable. Results for TDRS-3 are shown in Fig 11 and indicate that it appears to be stable. Results for NILESAT 101 are shown in Fig 12 and exhibit an unstable signature.

The spectrogram is a useful tool for observing a change in stability and serves as a cueing mechanism to initiate longer collections to confirm the behavior. We also saw some signatures that we didn't anticipate and can't explain. Fig. 13 shows a SL 12 R/B (2) (SSN 24897) signature. It's a slow GEO drift orbit, but shows all the signature characteristics of a stable object. Over 16 SL 12 R/B objects have shown a strong stable signature and 300+ others have a weaker signature that is similar.

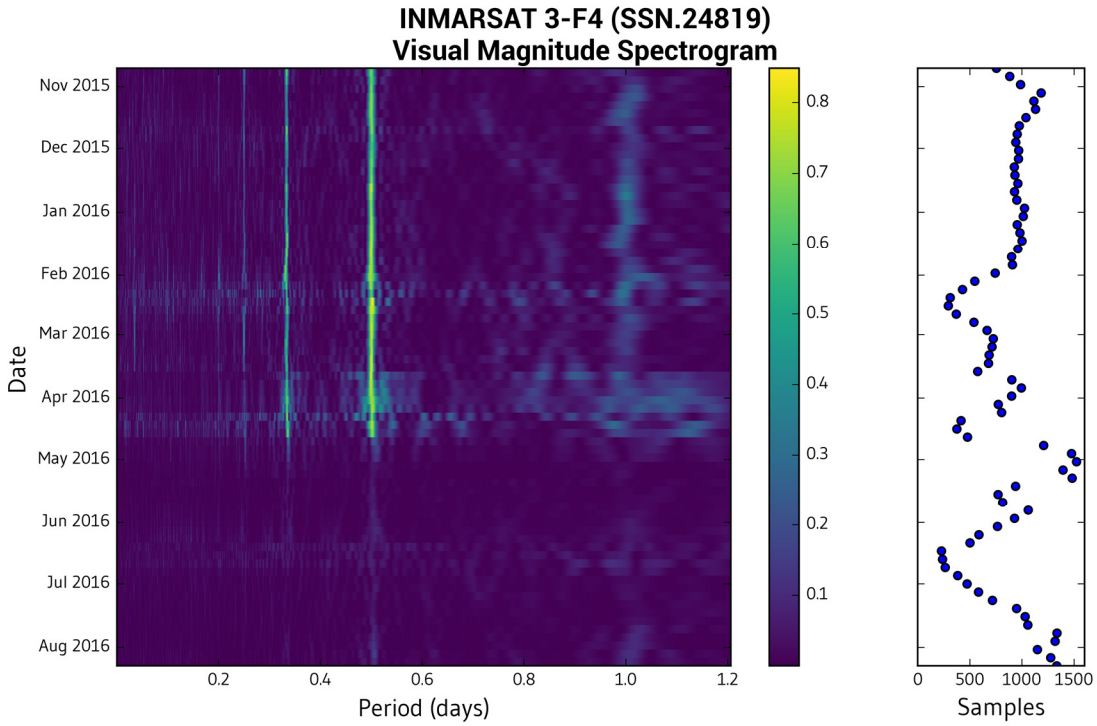

Fig. 10. INMARSAT 3-F4 Spectrogram

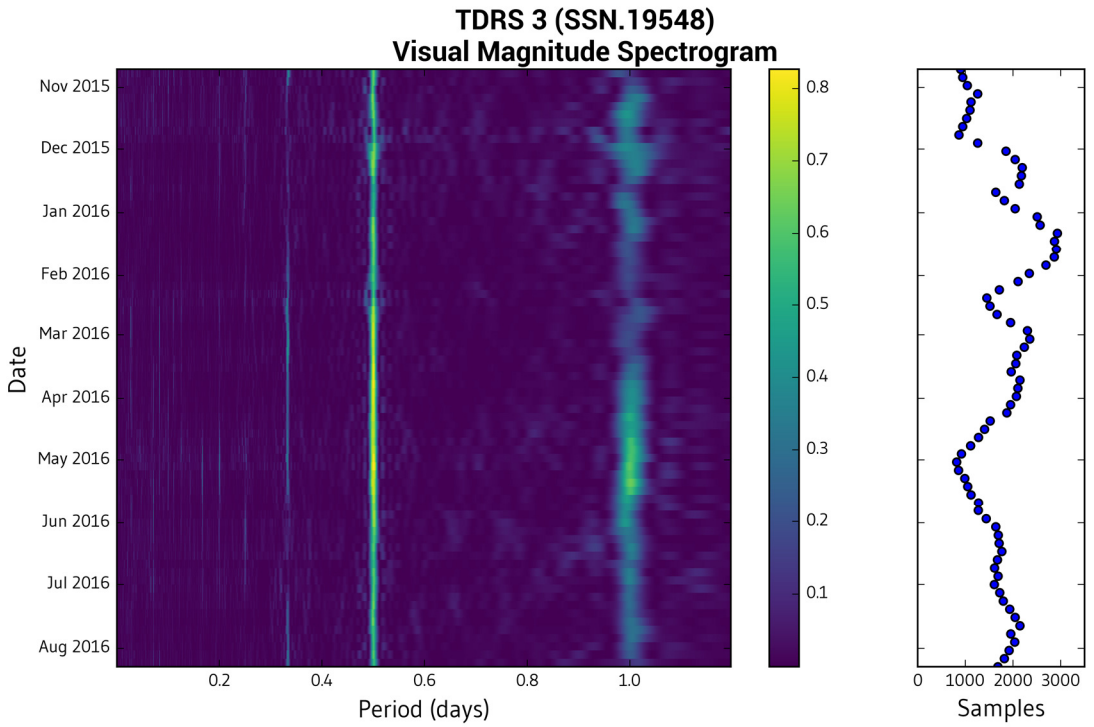

Fig. 11. TDRS-3 Spectrogram

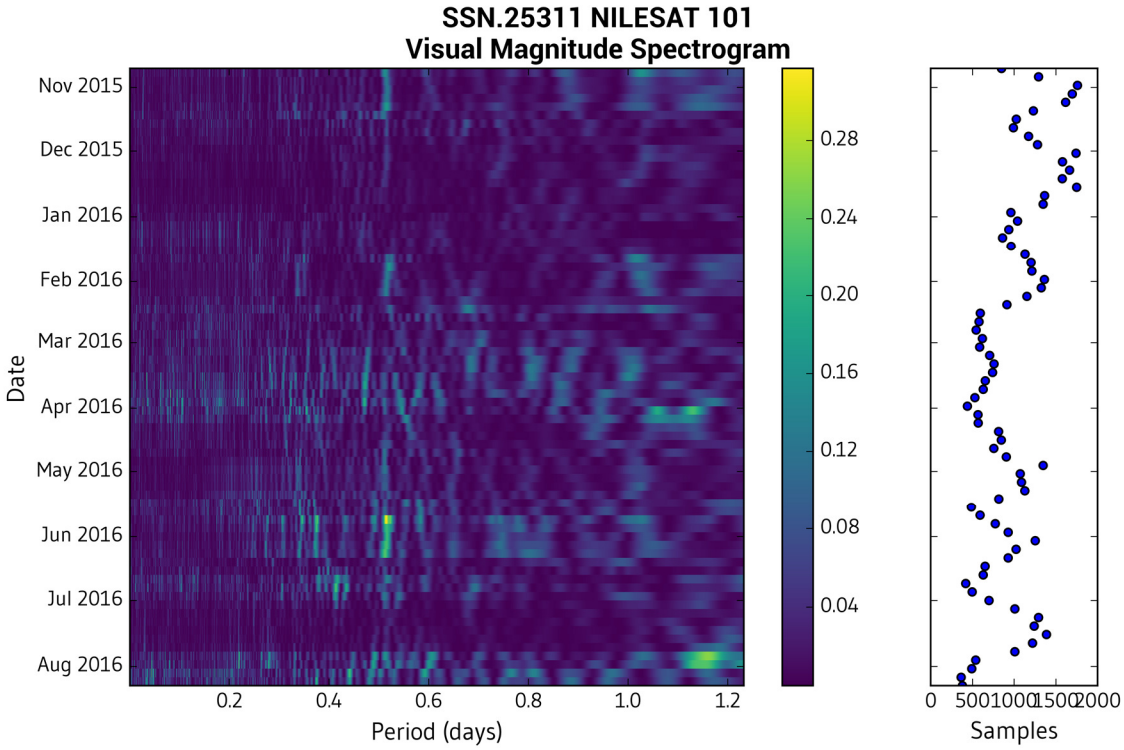

Fig. 12. NILESAT 101 Spectrogram

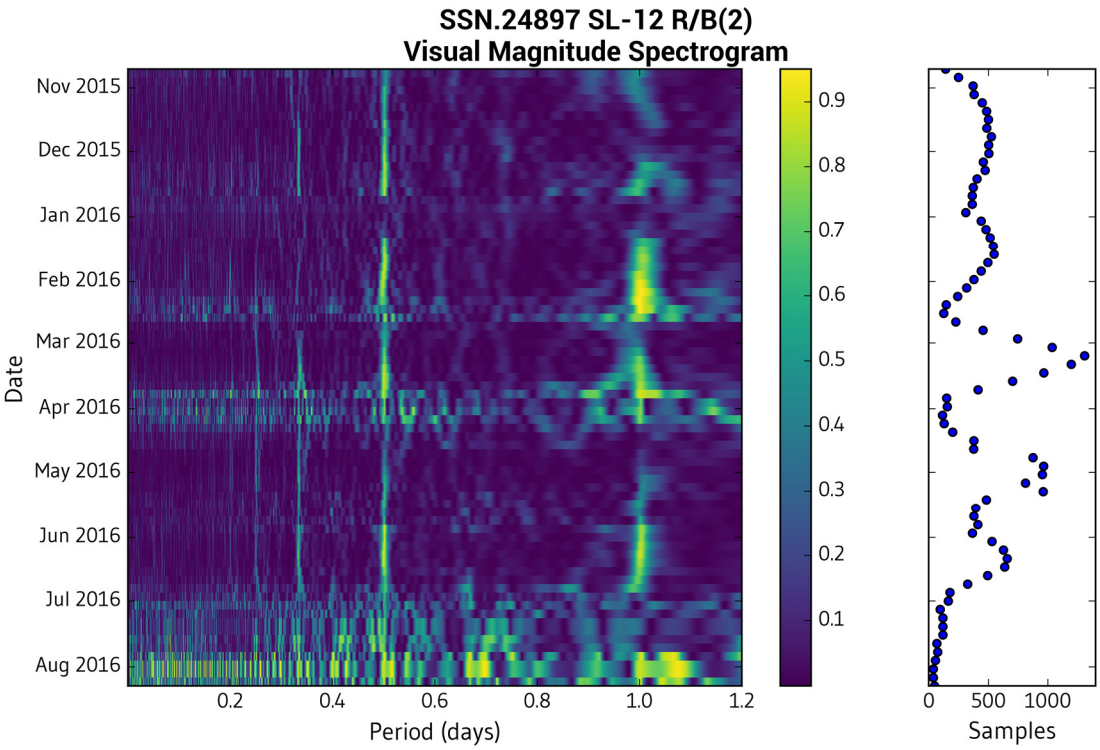

Fig. 13. SL 12 R/B (2) Spectrogram

5. CONCLUSIONS

Our analysis shows that it is possible to perform satellite stability assessment across a large number of objects and detect changes. We think this is a useful technique for identifying RSOs for additional follow up to perform a more detailed stability analysis using longer collections. Our next steps are to automate the change detection process and perform a more detailed simulation using 3D models, material properties, and synthetic scene creation. The optical data in the ComSpOC is primarily focused on objects in GEO, supersync GEO, and GEO crossing orbits. We are currently in the process of characterizing the stability of each object to assemble catalog wide statistics.

6. REFERENCES

1. https://mostlymissiledefense.com/2012/08/21/space-surveillance-the-visual-brightenss-and-size-of-space-objects-august-21-2012/, Retrieved March 03, 2016.
2. Cognion, R., “Observations and Modeling of GEO Satellites at Large Phase Angles”, Advanced Maui Optical and Space Surveillance Technologies Conference; Maui, HI, 2013.
3. Binz, C.R, Davis, M. A., Kelm, B. E., Moore, C. I., “Optical Survey of the Tumble Rates of Retired GEO Satellites”, Advanced Maui Optical and Space Surveillance Technologies Conference; Maui, HI, 2014.
4. Linder, E., Silha, J., Schildknect, T., Hager, M., “Extraction of Spin Periods of Space Debris from Optical Light Curves “; International Astronautical Congress 2015; Paper IAC-15- A6.1.2.
5. Poole, M., Murray-Krezan, J.; “Autonomous Object Characterization with Large Datasets”, Advanced Maui Optical and Space Surveillance Technologies Conference; Maui, HI, 2015.
6. Michael A. Earl and Gregg A. Wade. "Observations of the Spin-Period Variations of Inactive Box-Wing Geosynchronous Satellites", Journal of Spacecraft and Rockets, Vol. 52, No. 3 (2015), pp. 968-977.
7. Lomb, N. R.; “Least-Squares Frequency Analysis of Unequally Spaced Data”; Astrophysics and Space Science, vol. 39, Feb. 1976, p. 447-462.
8. Scargle, J. D.; “Studies in Astronomical Time Series Analysis. II – Statistical Aspects of Spectral Analysis of Unevenly Space Data”; Astrophysical Journal, Part 1, vol. 263, Dec. 15, 1982, p. 835-853.

9. Vio, R.; Diaz-Trigo, M.; Andreani, P., “Irregular Time Series in Astronomy and the use of the Lomb-Scargle periodogram”; Astronomy and Computing; Volume 1, February 2013.
10. VISIBLE MAGNITUDE OF TYPICAL SATELLITES IN SYNCHRONOUS ORBITS – KRAG